CrossMark

Vasopressin Impairment During Sepsis Is Associated with Hypothalamic Intrinsic Apoptotic Pathway and Microglial Activation

Luis Henrique Angenendt da Costa[1] · Nilton Nascimento dos Santos Júnior[1] ·
Carlos Henrique Rocha Catalão[1] · Tarek Sharshar[2] · Fabrice Chrétien[2] ·
Maria José Alves da Rocha[3]

Abstract Previous studies have shown that in the early phase of sepsis, the plasma concentration of arginine vasopressin (AVP) is increased, but in the late phase, its levels remain inadequately low, despite of persistent hypotension. One hypothesis suggested for this relative deficiency is apoptosis of vasopressinergic neurons. Here, we investigated apoptosis pathways in the hypothalamus during sepsis, as well as mechanisms underlying this process. Male Wistar rats were submitted to sepsis by cecal ligation and puncture (CLP) or nonmanipulated (naive) as control. After 6 and 24 h, the animals were decapitated and brain and blood were collected to assess hypothalamic apoptotic markers, IFN-γ plasma levels, and evidence for breakdown of the blood-brain barrier (BBB). Sepsis caused a decrease in mitochondrial antiapoptotic proteins (Bcl-2, Bcl-xL) in the hypothalamus, but had no effect on markers of cell death mediated by death receptors or immune cells. In the supraoptic nuclei of these animals, microglia morphology was consistent with activation, associated with an increase in plasma IFN-γ. A transitory breakdown of BBB in the hypothalamus was seen at 6 h following CLP. The results indicate that the intrinsic but not extrinsic apoptosis pathway is involved in the cell death observed in vasopressinergic neurons, and that this condition is temporally associated with microglial activation and BBB leaking.

Keywords Neuroendocrine dysfunction ·
Neuroinflammation · Blood-brain barrier · Cell death

Introduction

The pathophysiology of sepsis comprises a complex immunological response that, although essential to combat the infection, is also responsible for deleterious effects. The inflammatory agents produced by immune cells in the infection site or in the blood can directly or indirectly reach the central nervous system (CNS). There they can lead to a cerebral dysfunction denominated sepsis-associated encephalopathy (SAE), resulting in cognitive, autonomic, and endocrine impairment [1–3]. Regarding neuroendocrine changes during sepsis, our group has focused its investigation on arginine vasopressin (AVP) secretion, an important vasopressor peptide synthetized in the supraoptic (SON) and paraventricular (PVN) nuclei of the hypothalamus. By using cecal ligation and puncture as an experimental model of sepsis induction, we saw a drop in blood pressure and increase in plasma vasopressin following 4–6 h of surgery. However, 24 h after sepsis induction, the circulating levels of the hormone remain low, despite of persistent hypotension [4–8]. Moreover, at this time, we saw an impairment in magnocellular activation and increase in some markers of oxidative stress that could result in apoptosis of AVP-producing neurons [7, 9, 10].

Apoptosis, a form of programmed cell death, is an ATP-dependent highly complex process that comprises a sophisticated cascade of molecular events [11]. The key elements in apoptosis are caspases, a family of cysenil proteases that, once cleaved, become activated and initiate a proteolytic

✉ Maria José Alves da Rocha
  mjrocha@forp.usp.br

1 Department of Neurosciences and Behavioral Sciences, Ribeirão Preto Medical School, University of São Paulo, Ribeirão Preto, Brazil

2 Infection and Epidemiology Department, Institut Pasteur Human Histopathology and Animal Models Unit, Paris, France

3 Department of Morphology, Physiology and Basic Pathology, School of Dentistry of Ribeirão Preto, University of São Paulo, Avenida do Café s/n, CEP, Ribeirão Preto 14040-904, Brazil

cascade by activating other procaspases and amplifying the death signal [11, 12]. Caspase-3 is considered the most important effector caspase and is responsible for the final nuclear and cytoskeletal alterations. The intrinsic pathway that initiates apoptosis is essentially mitochondria-dependent. Several stimuli (radiation, hypoxia, nitric oxide, cytokines, etc.) cause an imbalance between proapoptotic (Bax, Bak, Bid, Bad, Bim) and antiapoptotic (Bcl-2, Bcl-xL, Bcl-w) proteins and allow mitochondrial cytochrome-c extravasation into the cytosol that, together with apoptotic protease activating factor 1 (Apaf-1), will activate caspase-9 to form the apoptosome and consequently cleave caspase-3 [13–15]. In contrast, the extrinsic pathway is triggered by the sensitization of cell surface death receptors (CD95, TNF-R1, TRAIL-R) by death ligands [16]. This binding results in the formation of a complex able to activate procaspase-8 and procaspase-10 that then can cleave caspase-3 [16, 17]. Cleaved caspase-8 can mediate a crosstalk with the intrinsic pathway by cleaving BH3 interacting-domain death agonist protein (Bid) and forming truncated Bid (tBID), which transduces apoptotic signals in mitochondria [18, 19]. Cell death can also be mediated by immune cells (cytotoxic CD8 T lymphocytes and natural killer cells) through exocytosis of perforin and granzymes that synergistically induce apoptosis in the target cell [20].

Previous studies from our laboratory showed that during sepsis, there is an augmented expression of cleaved caspase-3 and annexin-V affinity accompanied by a decrease in copeptin (a component of the AVP precursor) in SON and PVN, strongly suggesting that AVP-producing magnocellular neurons undergo apoptosis [9, 10]. With this in mind, we aimed to investigate which of the different apoptotic pathways plays a role in the hypothalamus of septic animals, and which mechanisms could be associated with the cell death process.

Material and Methods

Animals

Male Wistar rats (250–350 g) were used in the experiments. The animals were obtained from the Central Animal Facility at the University of São Paulo, Campus at Ribeirão Preto, and they were housed under temperature-controlled (25 ± 2 °C), and light-controlled (06:00–18:00) conditions, with free access to filtered water and a commercial balanced rodent diet. The experiments were carried out according to an Institutional Ethics Committee-approved protocol (CEUA protocol number 13.1.337.53.0).

Sepsis Induction

Sepsis was induced by cecal ligation and puncture (CLP) as described elsewhere [8–10]. Briefly, after deep sedation with tribromoethanol (250 mg/kg), the animals were submitted to a laparotomy. The cecum was exposed and ligated below the ileocecal valve and then punctured ten times with a 16-gauge needle. After a gentle squeeze for extravasation of feces, the cecum was returned to the peritoneal cavity and the incision was closed. Rats were given a subcutaneous injection of NaCl 0.9 % (5 mL/250 g body weight) for fluid resuscitation immediately after surgery. After the procedure, the animals were monitored for the presence of signs of infection (piloerection, tachypnea, lethargy). A mortality rate of around 60 % was observed 24 h after CLP. Nonmanipulated animals (naive) were used as control. Sixty-nine rats were used in this study.

Experimental Protocol

Control and septic rats were divided into three different groups at 6 h (early phase of sepsis) and 24 h (late phase of sepsis) following surgery. In the first one, the animals were decapitated for blood and brain collections. Blood was used for plasma INF-γ analysis and the brain for detection of apoptosis-related proteins expression in whole hypothalamus or in its supraoptic and paraventricular nuclei by western blot. The second group was perfused, and the brains were collected for immunofluorescence detection of cell death-related proteins and microglia analysis. The third group was separated for the investigation of blood-brain barrier permeability.

Western Blot

Whole hypothalamus or SON and PVN punches were homogenized in RIPA buffer (Sigma-Aldrich) containing a 10 % protease inhibitor cocktail (Sigma-Aldrich) and 0.5 % of phenylmethylsulfonyl fluoride (Sigma-Aldrich). Equal amounts (40 μg) of total protein were separated by SDS-PAGE in a 12 % polyacrylamide gel (125 V, 90 min). Following electrophoresis, proteins were blotted onto a nitrocellulose membrane (0.45 μm pore size; Millipore) in a tank blotting system (100 V, 120 min). The membranes were then kept in a blocking solution (BSA 5 % in PBS, with 0.2 % Tween 20) for 1 h and incubated overnight at 4 °C with primary antibodies targeting cleaved caspase-8 (IMGNEX, 1:2000), tBID (Millipore, 1:1500), CD8 (Santa Cruz, 1:2000), perforin (Santa Cruz, 1:500), granzyme B (Abcam, 1:1000), Bcl-2 (Santa Cruz, 1:1000), Bcl-xL (Abcam, 1:2000), and β-actin (Santa Cruz, 1:2000). Appropriate secondary HRP-conjugated antibodies (1:10,000 dilution) were incubated under agitation for 2 h at 4 °C. A chemiluminescence reaction kit (enhanced chemiluminescence [ECL], GE Healthcare) was used for detection of these proteins, which were visualized in a ChemiDoc MP System (BioRad) and analyzed by its respective software (ImageLab 5.2.1). The results were normalized against β-actin levels (internal control) of the samples.

Immunofluorescence

Free-floating sections (30 μm) were washed three times in PBS (0.01 M, 7, pH 7.4) and submitted to an antigen retrieval protocol. This included an incubation in Tris/EDTA (10 mM/ 1 mM, pH 9.0) solution for 5 min, followed by heating for 30 min in a water bath at 70 °C in 10 mM sodium citrate buffer (pH 6.0). After three new rinses with PBS, nonspecific binding sites were blocked for 60 min in PBS containing 5 % normal goat serum and 0.3 % Triton X-100. Subsequently, the sections were incubated for 24 h at 4 °C with specific antibodies: Iba-1 (WAKO, 1:1000), AVP (Peninsula, 1:10,000), HIF-1α (Santa Cruz, 1:50), cleaved caspase-3 (Cell Signaling, 1:400), and cytochrome-c (1:50, Santa Cruz Biotechnology). After rinsing again, the sections were incubated for 2 h at 4 °C with fluorescent conjugated antibodies (1:1000, goat anti-rabbit Alexa Fluor 594 conjugate or goat anti-mouse Alexa Fluor 488 conjugate, Life Technologies). Finally, the sections were mounted on gelatin-coated slides and covered with antifade mounting medium (ProLong® Gold Antifade Mountant, ThermoFisher Scientific) with DAPI, for nuclear staining. Images were captured using a Leica TCS-SP5 confocal microscope (Leica Microsystems).

Plasma Interferon-Gamma

Interferon-gamma (IFN-γ) plasma levels were measured by using a kit for specific enzyme-linked immunosorbent assay (ELISA) (ThermoFisher Scientific). The assays were performed following the manufacturer's instructions, and the detection limit was 2 pg/ml.

Blood-Brain Barrier Permeability

The integrity of the blood-brain barrier (BBB) was investigated using Evans blue dye extravasation 6 and 24 h after the CLP. Following sedation with TBE (250 mg/kg), the animals received an intravenous injection of 1 ml of Evan's blue solution (2 % w/v diluted in saline solution 0.9 %). After 1 h, the rats were perfused with 200 ml of 0.9 % saline solution and the brain was collected for hypothalamus dissection. Brain hemispheres or hypothalamic samples were homogenized in 50 % trichloroacetic acid, centrifuged at 3000× g at 4 °C during 20 min, and the supernatant was diluted in ethanol 1:1 (v/v). Evans blue content was measured by spectrophotometry (Synergy H1, Biotek) at 630 nm and quantified according to a standard curve. The results are presented as (ng of Evans blue stain/g of tissue).

Statistical Analysis

The data are presented as mean ± SEM. Cleaved caspase-8 and tBID data were analyzed using an unpaired Student's t test. Other variables with normal distribution were analyzed by one-way analysis of variance (ANOVA), followed by post hoc Tukey test. For those with nonparametrical distribution, a Kruskal-Wallis test was performed, followed by Dunn's post hoc test. Values of $p \leq 0.05$ were considered as significant.

Results

Hypothalamic Expression of Apoptosis Markers

Here, an evaluation of the different apoptosis pathways was performed. The analysis of the death receptor-mediated pathway in SON and PVN punches after 24 h following CLP did not show any significant difference in tBID and cleaved caspase-8 levels between the groups (Fig. 1). We also did not observe any effect on the levels of markers of immune cell-mediated cell death, such as CD8, granzyme B, and perforin in the hypothalamus of septic animals (Fig. 2). Regarding the mitochondrial pathway, protein levels of Bcl-xL were significantly decreased in the hypothalamus at 6 and 24 h ($p \leq 0.05$ in each group) and Bcl-2 levels at 24 h ($p \leq 0.05$) following sepsis (Fig. 3).

Immunostaining for HIF-1α, Cytochrome-c, and Cleaved Caspase-3 in Vasopressinergic Neurons

Immunolabeling for AVP and HIF-1α, cytochrome-c, and cleaved caspase-3 done in serial independent experiments showed increased staining for these markers in vasopressinergic neurons in the SON of septic animals at 24 h after surgery (Fig. 4). Labeling in control rats was absent or weak.

Glial Cell Analysis

Morphological evaluation of microglial cells (Fig. 5) by Iba-1 staining in the SON of control animals showed that these cells are ramified, with an oval and small cell body and long thin processes (Fig. 5a, b). In septic animals, these cells assumed an ameboid shape, with shortened processes and thick ramifications (Fig. 5c–e).

Plasma IFN-γ and BBB Permeability

Following 24 h after sepsis induction, we observed an increase ($p \leq 0.05$) in the plasma levels of IFN-γ, as shown in Fig. 6. While sepsis did not cause alterations in Evans blue permeability in the whole brain hemisphere at the two time points, it was clearly increased ($p \leq 0.05$) in the hypothalamus at the 6 h time point, but not at 24 h (Fig. 7).

Fig. 1 Western blot analysis (**a**) and quantification for cleaved caspase-8 (**b**, **c**) and tBID (**d**, **e**) in supraoptic (SON) and paraventricular (PVN) nuclei. There was no difference between naive (*white bar*) and septic (*dark bar*) animals at 24 h following sepsis induction by CLP. The data show means ± SEM of the expression ratio of cleaved caspase-8 or tBID normalized against β-actin. Statistical analysis was performed by using an unpaired Student's *t* test. *n* = 4–7 animals per group
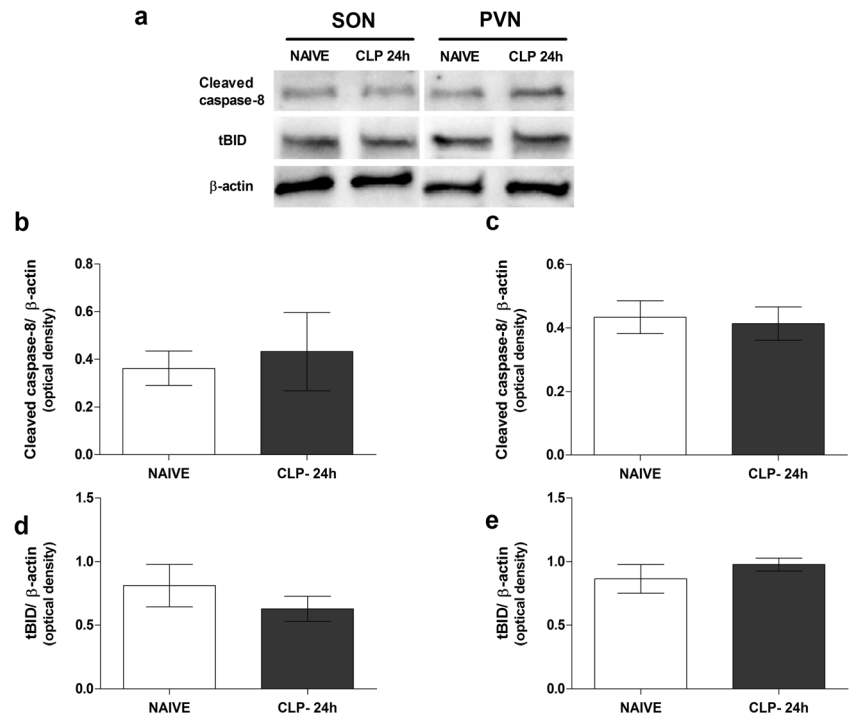
Discussion

The results here presented indicate that sepsis activated the intrinsic apoptotic pathway in the hypothalamus of CLP animals. This included increased immunolabeling of cell death markers in vasopressinergic neurons, associated with microglial activation and BBB disruption. An increase for these markers (cleaved caspase-3, cytochrome-c, HIF-1α) in the hypothalamus has previously been reported [9, 10, 21], but here, we show for the first time that this increase occurs specifically in AVP-producing magnocellular neurons. Even though we did not find evidence for the involvement of other apoptotic pathways in our experiments, we cannot discard the possibility that they may play a role posteriorly, as the disease progresses. In fact, in previous work, we saw that the increase in cleaved caspase-3 expression seen here at 24 h was also present at 48 h, even though there was no increase in cytochrome-c expression at that time point [9]. Cytotoxic lymphocytes may take even

Fig. 2 Western blot analysis (**a**) and quantification for immune-mediated cell death markers CD8 (**b**), granzyme B (**c**), and perforin (**d**) in hypothalamus. There was no difference in the levels of these markers comparing naive and septic (CLP) rats at 6 and 24 h after sepsis induction by CLP. The data show means ± SEM of the expression ratios between target proteins and β-actin. Statistical analysis was performed by one-way ANOVA followed by Tukey post hoc test. *n* = 5–7 per group
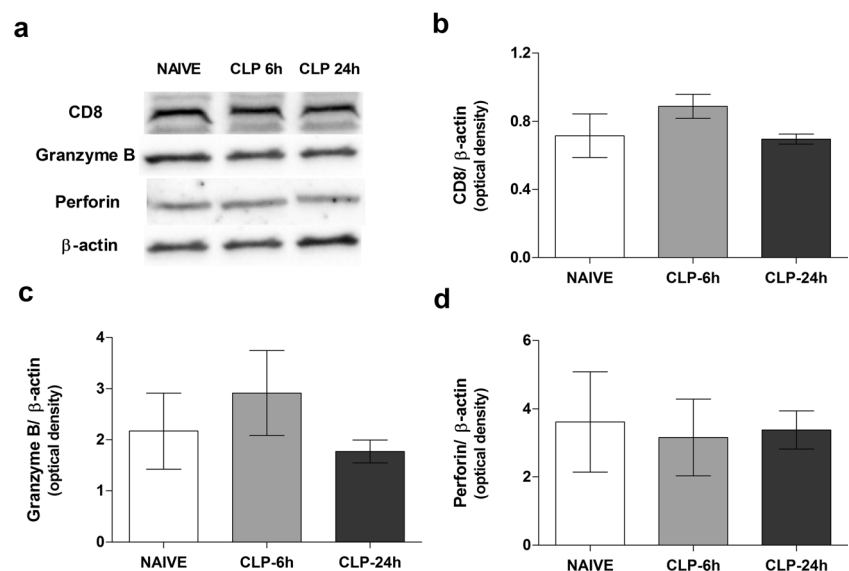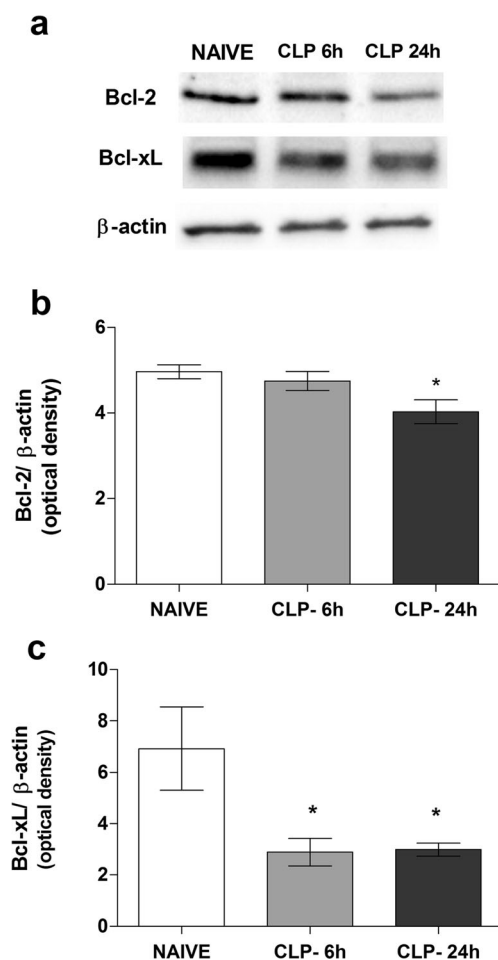
Fig. 3 Western blot analysis (**a**) and quantification for anti-apoptotic proteins showing difference in levels of Bcl-2 (**b**) and Bcl-xL (**c**) in the hypothalamus of naive and septic (CLP) animals at 6 and 24 h after sepsis induction. The data show means ± SEM of the expression ratios between target proteins and β-actin. Statistical analysis was performed by one-way ANOVA test followed by Tukey post hoc test; *$p \leq 0.05$ of CLP compared to naive group. $n = 6$–7 animals per group

Fig. 4 Photomicrographs illustrating immunofluorescence for AVP and HIF-1α (**a**), cytochrome-c (**b**), and cleaved caspase-3 (**c**) in coronal sections through the supraoptic nucleus (SON) of naive and septic (CLP) animals at 6 and 24 h following surgery. Images were obtained by confocal laser microscopy. Original magnification ×60 + ×3 optical zoom. *Scale bar* = 50 μm

more time, as their action depends on antigen processing and presentation by the major histocompatibility complex class 1 (MCH-1) to initiate the release of granzyme/perforin granules [22].

The decreased expression of hypothalamic Bcl-2 and Bcl-xL indicates that the mitochondrial pathway is already going through modifications. These antiapoptotic proteins act together in order to guarantee mitochondrial homeostasis, maintaining a stable permeability of the outer membrane. In fact, an overexpression of Bcl-2/Bcl-xL inhibits the translocation and oligomerization of the proapoptotic proteins Bax and Bak, preventing a loss of mitochondrial membrane potential and release of cytochrome-c into the cytosol [14, 23]. Bcl-xL is even more potent than Bcl-2 to inhibit this permeabilization [24], and its levels were diminished already
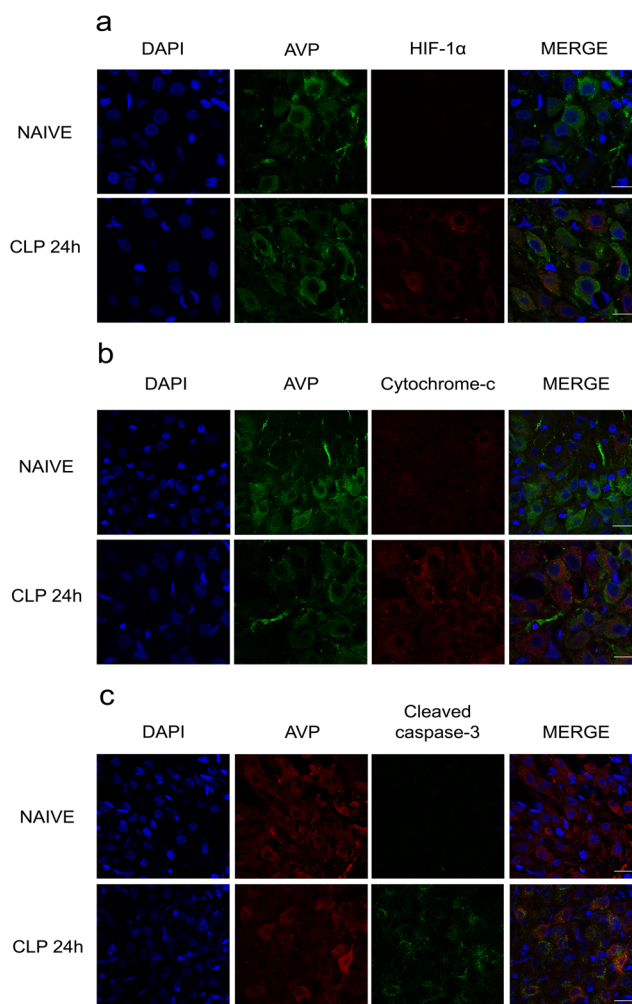
in the early phase of sepsis, as we could show here. Therefore, we infer that the hypothalamus may be vulnerable to cell death already in the initial stage of sepsis.

Inflammatory mediators play an important role in subsequent mechanisms of programmed death. Cytokines, notably interleukin-1β (IL-1β), can trigger the production of nitric oxide (NO) in the hypothalamus via the inducible isoform of NO synthase (iNOS) [25, 26]. In fact, a central injection of IL-1 receptor antagonist during sepsis leads to a reduction in NO levels in CSF and in hypothalamic NOS activity [8]. An increase in NO levels can affect mitochondrial bioenergetics, leading to a "metabolic hypoxia" state, which induces the expression and stability of the α subunit of hypoxia-induced factor 1 (HIF-1α) [27, 28]. The increased

Fig. 5 Photomicrographs illustrating Iba-1 immunostaining (*green*) in coronal sections through the supraoptic (SON) nucleus of naive and septic animals at 6 and 24 h. Cell nuclei were stained with DAPI (*blue*). Iba-1-positive cells in septic animals (**c–f**) showed larger cell bodies and shorter cell processes compared to the naive group (**a**, **b**), this indicating cell activation. Images were obtained by confocal laser microscopy. Original magnification ×60 (**a**, **c**, **e**); **b**, **d**, **f** magnifications (×3) of the original image. *Scale bar* = 50 μm
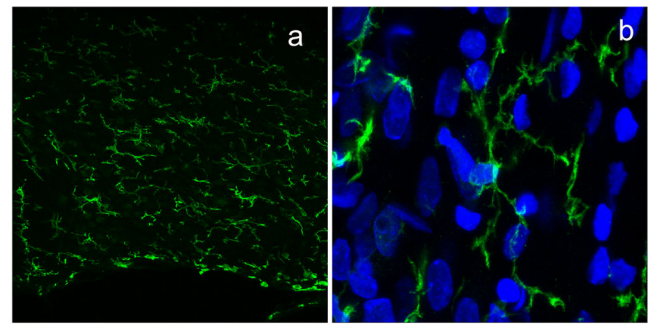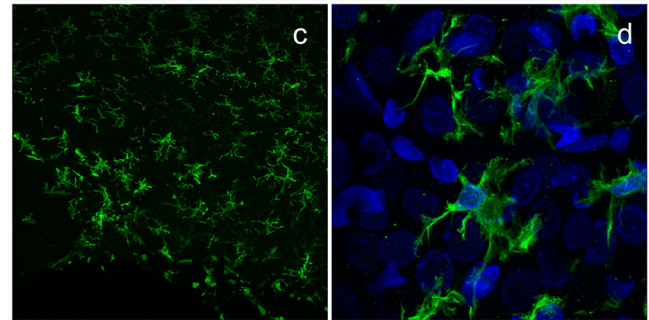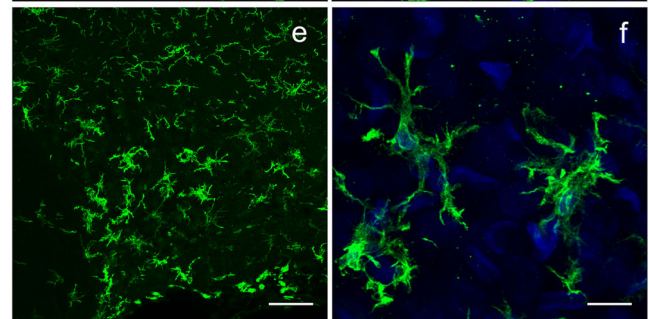
immunostaining for HIF-1α in vasopressinergic neurons during sepsis seen here indicates that they are under an abnormal bioenergetics condition. HIF-1 can promote gene activation and expression of Nip3, a proapoptotic
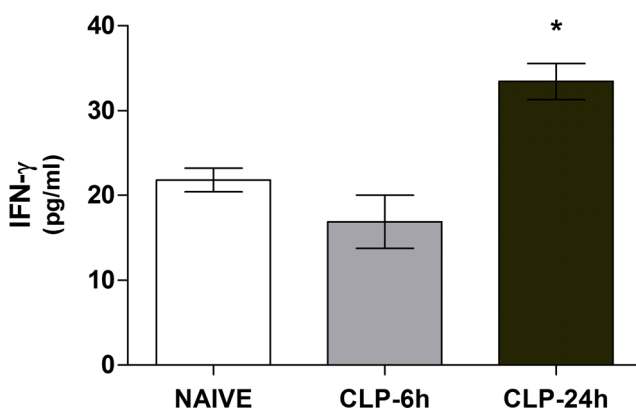

Fig. 6 Plasma levels of interferon-gamma in naive and septic (CLP) rats measured by ELISA. The data show means ± SEM. Statistical analysis was performed by one-way ANOVA followed by Tukey post hoc test; *$p \leq 0.05$ of CLP compared to naive group. $n = 6$–7 per group

protein that has been shown to sequester Bcl-2 and Bcl-xL and promote apoptosis [29].

Glial cells, which comprise microglia, astrocytes, oligodendrocytes, and ependymal cells, are known to be involved in several neurodegenerative conditions. Microglia activation can be recognized by changes in cell morphology: resting cells show long and thin ramifications, while activated ones present an ameboid shape, with short and thick processes [30, 31]. Our results showed that microglial cells in the SON of septic rats display a morphology compatible with activation. Interestingly, this was observed already at 6 h after CLP, then followed by an increase in IFN-γ plasma levels at 24 h. When stimulated by LPS or IFN-γ, microglia can assume a proinflammatory activated status and secrete neurotoxic molecules, like cytokines and NO [32]. Moreover, interleukin (IL)-1β, IL-6, and tumor necrosis factor-α (TNF-α) together with IFN-γ can promote a proinflammatory environment for microglia [33], and indeed, the levels of these cytokines are increased in this sepsis model [10]. There is evidence that microglia-derived IL-1β is responsible for inflammation
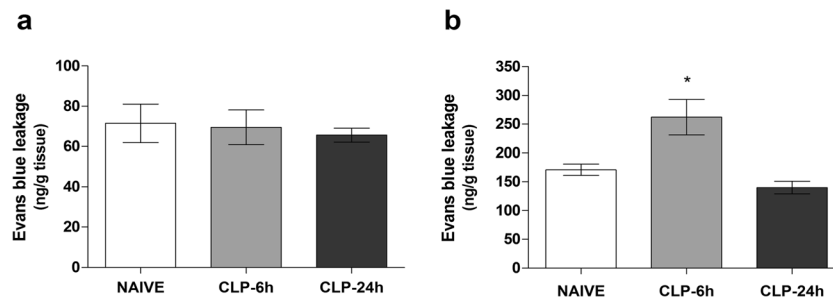
a

b

Fig. 7 BBB permeability (Evans blue assay) at 6 and 24 h after sepsis induction in whole brain hemisphere and hypothalamus. Data are presented as mean ± SEM. Statistical analysis was performed by one-

way ANOVA followed by Tukey post hoc test.*$p \leq 0.05$ of septic versus naive group. $n = 4$–7 rats per group

in the hippocampus and cerebral cortex and that this can cause cognitive and synaptic impairment during sepsis [34, 35]. Furthermore, in a previous work, we saw that when blocking the IL-1β pathway in the CNS, vasopressin secretion in the late phase of sepsis is improved, associated with a decreased expression of HIF-1 and procaspase-3 encoding genes, suggesting a reduction of apoptosis in vasopressinergic neurons [8, 21]. Therefore, microglia could be a source of inflammatory agents that are harmful for the hypothalamic-neurohypophyseal axis in systemic inflammation. Astrocyte activation can also be deleterious, but in our sepsis model, hypothalamus GFAP levels remained unaltered until 24 h (data not shown). Although these cells have an intimate crosstalk with microglia during neuroinflammatory conditions, their activation tends to be posterior [36].

Several experimental studies have shown impairment of the blood-brain barrier during sepsis [37–40]. This barrier represents a highly specialized structure that selectively regulates the communication between brain and systemic circulation, but under pathological conditions its breakdown can be mediated by TNF-α [41] and nitric oxide [42, 43]. Vasopressin is also associated with BBB damage [44, 45]. Here, we saw an increased hypothalamic Evans blue (EB) leakage at the same time (early phase of sepsis) when high vasopressin levels are detected. Even though it was not found any difference in EB extravasation at 24 h, as observed in other studies with sepsis [46, 47], slight variations in the CLP model (number of punctures, needle size) could induce a different kinetic in our animals. We believe that BBB breakdown permits circulating cytokines to reach the hypothalamus and contribute to or promote further direct or indirect (through microglial activation) neuronal damage that can culminate in the impairment of vasopressin secretion. Although we did not measure plasma AVP levels in this study, we previously reported [5, 7, 8] that there is an increase at 6 h followed by a return to basal levels at 24 h in the CLP-induced sepsis model.

Concluding, our results show that cell death of vasopressinergic neurons is mediated by the intrinsic but not extrinsic apoptosis pathway, and that this process is associated with local microglial activation and BBB damage.

Compliance with Ethical Standards This study involves the use of rats. All animal experiments in this study were carried out according to an Institutional Ethics Committee-approved protocol (CEUA protocol number 13.1.337.53.0).

Conflict of Interest The authors declare that they have no conflict of interest.

References

1. McCann SM, Kimura M, Karanth S, WH Y, Mastronardi CA, Rettori V (2000) The mechanism of action of cytokines to control the release of hypothalamic and pituitary hormones in infection. Ann N Y Acad Sci 917:4–18
2. Kovács KJ (2002) Neurohypophyseal hormones in the integration of physiological responses to immune challenges. Prog Brain Res 139:127–146
3. Sonneville R, Verdonk F, Rauturier C, Klein IF, Wolff M, Annane D, et al. (2013) Understanding brain dysfunction in sepsis. Ann Intensive Care 3:15
4. Pancoto JA, Corrêa PB, Oliveira-Pelegrin GR, Rocha MJ (2008) Autonomic dysfunction in experimental sepsis induced by cecal ligation and puncture. Auton Neurosci 138:57–63
5. Oliveira-Pelegrin GR, Ravanelli MI, Branco LG, Rocha MJ (2009) Thermoregulation and vasopressin secretion during polymicrobial sepsis. Neuroimmunomodulation 16:45–53
6. Oliveira-Pelegrin GR, de Azevedo SV, Yao ST, Murphy D, Rocha MJ (2010) Central NOS inhibition differentially affects vasopressin gene expression in hypothalamic nuclei in septic rats. J Neuroimmunol 227:80–86

7. Corrêa PB, Pancoto JA, de Oliveira-Pelegrin GR, Cárnio EC, Rocha MJ (2007) Participation of iNOS-derived NO in hypothalamic activation and vasopressin release during polymicrobial sepsis. J Neuroimmunol 183:17–25

8. Wahab F, Tazinafo LF, Cárnio EC, Aguila FA, Batalhão ME, Rocha MJ (2015) Interleukin-1 receptor antagonist decreases cerebrospinal fluid nitric oxide levels and increases vasopressin secretion in the late phase of sepsis in rats. Endocrine 49:215–221

9. Oliveira-Pelegrin GR, Basso PJ, Rocha MJ (2014) Cellular bioenergetics changes in magnocellular neurons may affect copeptin expression in the late phase of sepsis. J Neuroimmunol 267:28–34

10. Oliveira-Pelegrin GR, Basso PJ, Soares AS, Martinez MR, Riester KD, Rocha MJ (2013) Cleaved caspase-3 expression in hypothalamic magnocellular neurons may affect vasopressin secretion during experimental polymicrobial sepsis. J Neuroimmunol 258:10–16

11. Elmore S (2007) Apoptosis: a review of programmed cell death. Toxicol Pathol 35:495–516

12. Aziz M, Jacob A, Wang P (2014) Revisiting caspases in sepsis. Cell Death Dis 5:e1526

13. Hengartner MO (2000) The biochemistry of apoptosis. Nature 407:770–776

14. Kim R (2005) Unknotting the roles of Bcl-2 and Bcl-xL in cell death. Biochem Biophys Res Commun 333:336–343

15. Snyder CM, Shroff EH, Liu J, Chandel NS (2009) Nitric oxide induces cell death by regulating anti-apoptotic BCL-2 family members. PLoS One 4:e7059

16. Lavrik IN (2014) Systems biology of death receptor networks: live and let die. Cell Death Dis 5:e1259

17. Kruidering M, Evan GI (2000) Caspase-8 in apoptosis: the beginning of "the end"? IUBMB Life 50:85–90

18. Li H, Zhu H, Xu CJ, Yuan J (1998) Cleavage of BID by caspase 8 mediates the mitochondrial damage in the Fas pathway of apoptosis. Cell 94:491–501

19. Gross A, Yin XM, Wang K, Wei MC, Jockel J, Milliman C, et al. (1999) Caspase cleaved BID targets mitochondria and is required for cytochrome c release, while BCL-XL prevents this release but not tumor necrosis factor-R1/Fas death. J Biol Chem 274:1156–1163

20. Trapani JA, Smyth MJ (2002) Functional significance of the perforin/granzyme cell death pathway. Nat Rev Immunol 2:735–747

21. Wahab F, Santos-Junior NN, de Almeida Rodrigues RP, Costa LH, Catalão CH, Rocha MJ (2015) Interleukin-1 receptor antagonist decreases hypothalamic oxidative stress during experimental sepsis. Mol Neurobiol. doi:10.1007/s12035-015-9338-4

22. Ryan SO, Cobb BA (2012) Roles for major histocompatibility complex glycosylation in immune function. Semin Immunopathol 34:425–441

23. Leber B, Lin J, Andrews DW (2010) Still embedded together binding to membranes regulates Bcl-2 protein interactions. Oncogene 29:5221–5230

24. Keogh SA, Walczak H, Bouchier-Hayes L, Martin SJ (2000) Failure of Bcl-2 to block cytochrome c redistribution during TRAIL-induced apoptosis. FEBS Lett 471:93–98

25. Wong ML, Rettori V, al-Shekhlee A, Bongiorno PB, Canteros G, McCann SM, et al. (1996) Inducible nitric oxide synthase gene expression in the brain during systemic inflammation. Nat Med 2:581–584

26. Wong ML, Bongiorno PB, Rettori V, McCann SM, Licinio J (1997) Interleukin (IL) 1beta, IL-1 receptor antagonist, IL-10, and IL-13 gene expression in the central nervous system and anterior pituitary during systemic inflammation: pathophysiological implications. Proc Natl Acad Sci U S A 94:227–232

27. Mander P, Brown GC (2004) Nitric oxide, hypoxia and brain inflammation. Biochem Soc Trans 32:1068–1069

28. Erusalimsky JD, Moncada S (2007) Nitric oxide and mitochondrial signaling: from physiology to pathophysiology. Arterioscler Thromb Vasc Biol 27:2524–2531

29. Bruick RK (2000) Expression of the gene encoding the proapoptotic Nip3 protein is induced by hypoxia. Proc Natl Acad Sci U S A 97:9082–9087

30. Kettenmann H, Hanisch UK, Noda M, Verkhratsky A (2011) Physiology of microglia. Physiol Rev 91:461–553

31. Morrison HW, Filosa JA (2013) A quantitative spatiotemporal analysis of microglia morphology during ischemic stroke and reperfusion. J Neuroinflammation 10:4

32. Eggen BJ, Raj D, Hanisch UK, Boddeke HW (2013) Microglial phenotype and adaptation. J NeuroImmune Pharmacol 8:807–823

33. Basu A, Krady JK, Enterline JR, Levison SW (2002) Transforming growth factor beta1 prevents IL-1beta-induced microglial activation, whereas TNFalpha- and IL-6-stimulated activation are not antagonized. Glia 40:109–120

34. Moraes CA, Santos G, Spohr TC, D'Avila JC, Lima FR, Benjamim CF, et al. (2014) Activated microglia-induced deficits in excitatory synapses through IL-1β: implications for cognitive impairment in sepsis. Mol Neurobiol 52:653–663

35. Mina F, Comim CM, Dominguini D, Cassol-Jr OJ, Dall Igna DM, Ferreira GK, et al. (2014) Il1-β involvement in cognitive impairment after sepsis. Mol Neurobiol 49:1069–1076

36. Liu W, Tang Y, Feng J (2011) Cross talk between activation of microglia and astrocytes in pathological conditions in the central nervous system. Life Sci 89:141–146

37. Flierl MA, Rittirsch D, Weckbach S, Huber-Lang M, Ipaktchi K, Ward PA, et al. (2011) Disturbances of the hypothalamic-pituitary-adrenal axis and plasma electrolytes during experimental sepsis. Ann Intensive Care 1:53

38. Nishioku T, Dohgu S, Takata F, Eto T, Ishikawa N, Kodama KB, et al. (2009) Detachment of brain pericytes from the basal lamina is involved in disruption of the blood-brain barrier caused by lipopolysaccharide-induced sepsis in mice. Cell Mol Neurobiol 29:309–316

39. Cardoso FL, Kittel A, Veszelka S, Palmela I, Tóth A, Brites D, et al. (2012) Exposure to lipopolysaccharide and/or unconjugated bilirubin impair the integrity and function of brain microvascular endothelial cells. PLoS One 7:e35919

40. Michels M, Danielski LG, Vieira A, Florentino D, Dall'Igna D, Galant L, et al. (2015) CD40-CD40 ligand pathway is a major component of acute neuroinflammation and contributes to long-term cognitive dysfunction after sepsis. Mol Med 21:219–226

41. Candelario-Jalil E, Taheri S, Yang Y, Sood R, Grossetete M, Estrada EY, et al. (2007) Cyclooxygenase inhibition limits blood-brain barrier disruption following intracerebral injection of tumor necrosis factor-alpha in the rat. J Pharmacol Exp Ther 323:488–498

42. Minami T, Okazaki J, Kawabata A, Kawaki H, Okazaki Y, Tohno Y (1998) Roles of nitric oxide and prostaglandins in the increased permeability of the blood-brain barrier caused by lipopolysaccharide. Environ Toxicol Pharmacol 5:35–41

43. Boje KM, Lakhman SS (2000) Nitric oxide redox species exert differential permeability effects on the blood-brain barrier. J Pharmacol Exp Ther 293:545–550

44. Manaenko A, Fathali N, Khatibi NH, Lekic T, Hasegawa Y, Martin R, et al. (2011) Arginine-vasopressin V1a receptor inhibition improves neurologic outcomes following an intracerebral hemorrhagic brain injury. Neurochem Int 58:542–548

45. Zeynalov E, Jones SM, Seo JW, Snell LD, Elliott JP (2015) Arginine-vasopressin receptor blocker Conivaptan reduces brain edema and blood-brain barrier disruption after experimental stroke in mice. PLoS One 10:e0136121

46. Dal-Pizzol F, Rojas HA, dos Santos EM, et al. (2013) Matrix metalloproteinase-2 and metalloproteinase-9 activities are associated with blood-brain barrier dysfunction in an animal model of severe sepsis. Mol Neurobiol 48:62–70

47. Comim CM, Vilela MC, Constantino LS, et al. (2011) Traffic of leukocytes and cytokine up-regulation in the central nervous system in sepsis. Intensive Care Med 37:711–718